Pan *Nanoscale Research Letters* (2016) 11:113
DOI 10.1186/s11671-016-1329-5

Nanoscale Research Letters
a SpringerOpen Journal

NANO EXPRESS Open Access

Tension-Enhanced Hydrogen Evolution Reaction on Vanadium Disulfide Monolayer

Hui Pan

Abstract

Water electrolysis is an efficient way for hydrogen production. Finding efficient, cheap, and eco-friendly electrocatalysts is essential to the development of this technology. In the work, we present a first-principles study on the effects of tension on the hydrogen evolution reaction of a novel electrocatalyst, vanadium disulfide (VS_2) monolayer. Two electrocatalytic processes, individual and collective processes, are investigated. We show that the catalytic ability of VS_2 monolayer at higher hydrogen coverage can be efficiently improved by escalating tension. We find that the individual process is easier to occur in a wide range of hydrogen coverage and the collective process is possible at a certain hydrogen coverage under the same tension. The best hydrogen evolution reaction with near-zero Gibbs free energy can be achieved by tuning tension. We further show that the change of catalytic activity with tension and hydrogen coverage is induced by the change of free carrier density around the Fermi level, that is, higher carrier density, better catalytic performance. It is expected that tension can be a simple way to improve the catalytic activity, leading to the design of novel electrocatalysts for efficient hydrogen production from water electrolysis.

Keywords: VS_2 monolayer, Hydrogen evolution reduction, Water electrolysis, Tension, First-principles calculation

Background

Hydrogen, as an important energy carrier, is considered as a replacement of fossil fuels because of its abundant, clean, and renewable characteristics [1, 2]. Hydrogen production can be realized by photo-driven or electrical-driven water splitting [3–7], stream reforming [8], natural gas oxidization [9], carbonation [10], biomass electrolysis [11, 12], etc. Among these methods, catalytic water-spitting is highly appreciated because it is the cleanest way for hydrogen production, where hydrogen is evolving from proton to gas molecule by reduction [3–7]. Especially, electrical-driven water electrolysis has attracted increasing interests because of its high efficiency and eco-friendliness [7, 13–15]. To improve production efficiency and reduce cost, the design and fabrication of highly active, stable, and cheap electrocatalysts are critical to the development of green energy technology. It is well-known that noble metals and their alloys, such as platinum, are the most efficient catalysts in water electrolysis [16–22]. However, large-scale application of these catalysts in hydrogen evolution reaction (HER) for hydrogen production is difficult because they are rare and expensive. Alternatively, finding novel, environmental-friendly electrocatalysts with earth-abundant elements has been carried out with considerable efforts [7, 15].

Recently, transition metal dichalcogenides (TMDs) nanomaterials have been widely investigated as electrocatalysts in water electrolysis [23–32]. Particularly, The TMD monolayers with the formula of MX_2, which has a sandwiched structure with one M-atom (M = transition metal element) layer enclosed within two X layers (X = chalcogen element), and the atoms in layers are hexagonally packed, have attracted increasing attention because of their high surface area, active edges states, and high mechanic flexibility [15, 25, 30–40]. For example, MX_2 nanoribbons show high HER performance in water electrolysis due to their metallic edges [31], which can be further improved by edge doping and substrate [41, 42]. Metallic WS_2 monolayers showed better HER performance than semiconducting counterpart [38]. Recently, Pan reported that VS_2 monolayer shows excellent HER activity [32]. However, its performance is reduced at high hydrogen coverage because

Correspondence: huipan@umac.mo
Institute of Applied Physics and Materials Engineering, Faculty of Science and Technology, University of Macau, Macao SAR, China

of reduced conductivity. To improve the HER performance of TMDs monolayers, the basic principle for the design of catalysts is to achieve a near-zero overpotential [18]. It has been reported that the improvement of HER activity can be achieved by doping, forming defect, and hybridizing with graphene [15, 23–42]. Voiry et al. [38] and Lee et al. [43] reported that mechanic strain can efficiently improve the HER activity of WS_2 and MoS_2 monolayers. To date, the effect of strain on the HER performance of TMDs monolayers at various hydrogen coverages and strength of tension has not been systematically studied. In this work, we carry out first-principles study on the improvement of the HER performance of VS_2 monolayer with tension. We show that the improvement of catalytic activity of VS_2 monolayer strongly depends to the strength of applied tension, hydrogen coverage, and reaction process. We find that the catalytic performance at higher hydrogen coverage can be enhanced by increasing tension, and both individual/collective processes can happen at the same tension depending on hydrogen coverage. We further show that the catalytic performance is closely related to free carrier density, which is controlled by the tension and hydrogen coverage.

Methods

First-principles calculations on the basis of the density functional theory (DFT) [44] and the Perdew-Burke-Eznerhof generalized gradient approximation (PBE-GGA) [45] are carried out to study the effect of tension on the HER activity of VS_2 monolayer. The Vienna ab initio simulation package (VASP) [46] with projector augmented wave (PAW) scheme [47, 48] is used in our calculations. The Monkhorst and Pack scheme of k point sampling ($3 \times 3 \times 1$) is used for integration over the first Brillouin zone [49] and the cut-off energy is 450 eV. A sufficiently large supercell with $4 \times 4 \times 1$ unit cells and a vacuum region of at least 20 Å in the vertical direction is used to investigate the hydrogen-coverage-dependent HER performance and avoid the interaction between images in neighboring cells (Fig. 1). Good convergence is obtained with these parameters and the total energy is converged to 2.0×10^{-5} eV/atom.

Results and Discussion

The larger supercell with $4 \times 4 \times 1$ unit cells is constructed based on the unit of VS2 monolayer with one surface fully covered by hydrogen atoms, that is, one S atom is bonded with one H atom on one side of the monolayer [50]. The hexagonal supercell with a lattice constant of 13.1 Å (a0) has 16 H, 32 S, and 16 V atoms (Fig. 1). To investigate the effect of tension on its HER performance, the lattice is statically extended from a_0 to a by biaxial stretching or tension $\left(\varepsilon = \frac{a-a_0}{a_0} \times 100\,\%\right)$. The calculation on H-coverage-dependent HER performance is carried out by removing hydrogen atoms one by one from the surface. The H-coverage is defined as $\frac{n}{16}$ ($n = 0 \sim 16$). On the basis of the Sabatier principle, the HER performance of electrocatalyst in water electrolysis can be quantified by calculating the reaction free energy of hydrogen adsorption (ΔGH) [18, 19, 32, 33, 38], which can be obtained from following formula:

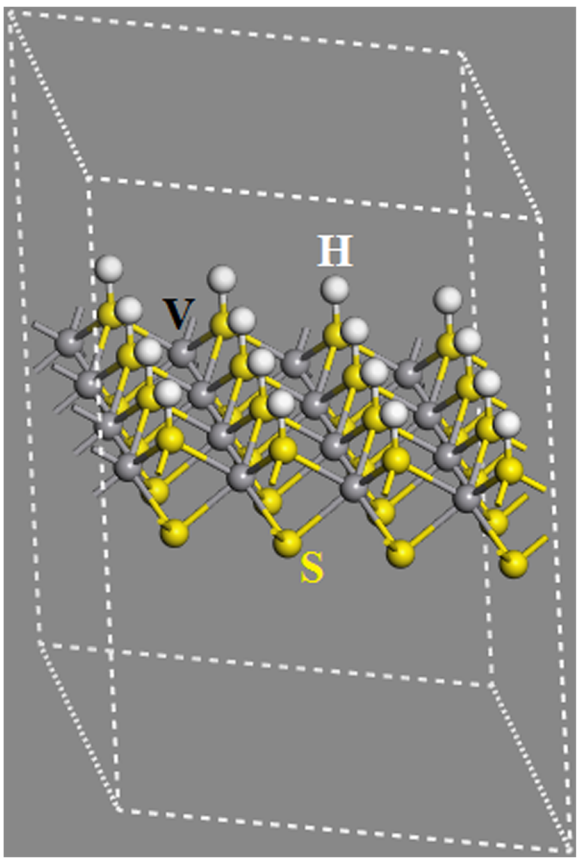

Fig. 1 Atomic structure of VS_2 monolayer with one surface fully covered by hydrogen atoms

$$\Delta G_{\mathrm{H}} = \Delta E_{\mathrm{H}} + \Delta E_{\mathrm{ZPE}} - T\Delta S_{\mathrm{H}} \tag{1}$$

where ΔE_{H} is the H-coverage-dependent hydrogen chemisorption energy. It can be differential chemisorption energy as calculated by:

$$\Delta E_{\mathrm{H}} = E(\mathrm{VS_2} + n\mathrm{H}) - E(\mathrm{VS_2} + (n-1)\mathrm{H}) - \frac{1}{2}E(\mathrm{H_2}) \tag{2}$$

or it can be average chemisorption energy calculated by

$$\Delta E_{\mathrm{H}} = \left(E(\mathrm{VS_2} + n\mathrm{H}) - E(\mathrm{VS_2}) - \frac{n}{2}E(\mathrm{H_2})\right)/n \qquad (3)$$

where n is the number of H atoms adsorbed on a VS_2 monolayer under tension. The H-coverage-dependent ΔG_H can be obtained by changing n. $E(VS_2 + nH)$, $E(VS_2)$, and $E(H_2)$ in Eqs. (2 and 3) are the energies of monolayer with hydrogen atoms (n), pure VS_2 monolayer, and hydrogen molecule, respectively. ΔS_H is the difference in entropy. ΔE_{ZPE} is the difference in zero point energy between the adsorbed and the gas phase. $\Delta E_{ZPE} - T\Delta S_H$ is about 0.24 eV [18, 19]. Therefore, Eq. (1) can be simplified to $\Delta G_H = \Delta E_H + 0.24$. According to the two methods (Eqs. 2 and 3) for the calculation of hydrogen chemisorption energy, the reaction free energies can be defined as differential ΔG_H (d-ΔG_H) and average ΔG_H (a-ΔG_H), which can be used to express the hydrogen production in the individual and collective processes, respectively. The individual process describes that hydrogen is produced one by one, while the collective process shows that all of hydrogen atoms on the surface are simultaneously converted to molecules. It is required that electrocatalyst with optimal HER performance should have a ΔG_H near 0 eV.

Our first-principles calculations show that ΔG_H is dependent on the H-coverage and can be efficiently tuned by applied tension (Fig. 2). We see that the trend of d-ΔG_H as a function of hydrogen coverage under tension is almost similar to that without tension in the individual process (ΔE_H is calculated from Eq. 2), that is, d-ΔG_H increases as hydrogen coverage increases [32]. Importantly, d-ΔG_H is reduced upon the tension applied and the HER activity of VS_2 monolayer in individual process at certain hydrogen coverage is improved by tension. The VS_2 monolayer under $\varepsilon = 2$ % shows best HER performance in individual process with d-ΔG_H equal to −0.043 and −0.029 eV at the hydrogen coverages of $\frac{2}{16}$ and $\frac{3}{16}$, respectively (Fig. 2a). Under $\varepsilon = 6$ %, the best HER performance occurs at the hydrogen coverages of $\frac{4}{16}$ and $\frac{5}{16}$ with d-ΔG_H equal to 0.023 and 0.018 eV, respectively (Fig. 2a). Further increasing ε to 10 %, the VS_2 monolayer shows best HER activity at the hydrogen coverages of $\frac{6}{16}$, $\frac{7}{16}$, and $\frac{9}{16}$ (d-ΔG_H = 0.024, 0.040, and −0.027 eV) (Fig. 2a). Clearly, the HER activity of VS_2 monolayer in individual process is improved at relatively high H-coverage as tension increases, while that at low H-coverage is weakened. At the same time, we see that the effect of tension on the HER activity at full H-coverage $\left(\frac{16}{16}\right)$ is minor in the individual process (Fig. 2a), because removing one hydrogen atom is subjected to the strong attraction from the remained hydrogen atoms. Compared to the individual process, a-ΔG_H in the collective process (ΔE_H is calculated from Eq. 3) increases smoothly as the H-coverage increases (Fig. 2b). The best HER activity of VS_2 monolayer with a-ΔG_H near zero (−0.007 eV) occurs at a hydrogen coverage of $\frac{5}{16}$ under $\varepsilon = 2$ %. Under $\varepsilon = 6$ %, the optimal performance (a-ΔG_H = −0.005~0.02 eV) is within a H-coverage range from $\frac{8}{16}$ to $\frac{10}{16}$. Further increasing tension to 10 %, VS_2 monolayer is more active at a H-coverage of around $\frac{14}{16}$ (a-ΔG_H = −0.016 eV). Interestingly, ΔG_H in the collective process at full hydrogen coverage is significantly reduced upon the tension applied, which is about 0.1 eV/H at $\varepsilon = 10$ % (Fig. 2b). Although the absolute value of a-ΔG_H in the collective process is smaller than that in the individual process at full H-coverage, it should be difficult to happen if considering the total number of H atoms. By comparing the individual and collective processes (Fig. 2), we see that individual process is easier than collective process because absolute value of d-ΔG_H is smaller than that of a-ΔG_H multiplied by the number of H atoms on the surface of the monolayer. However, the collective process prefers

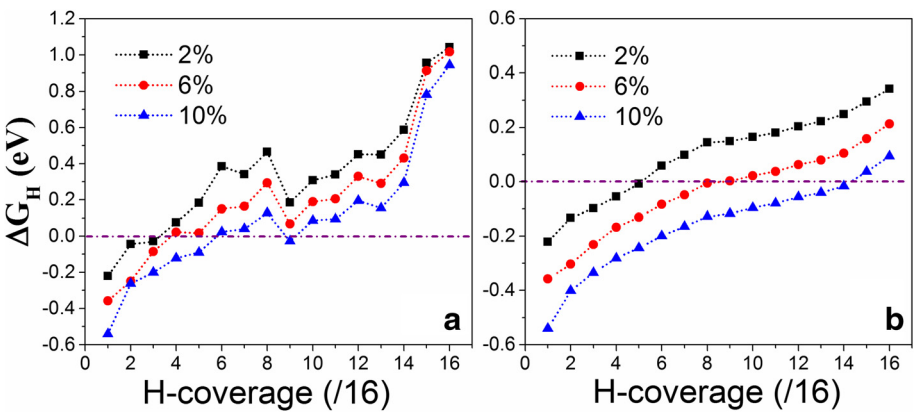

Fig. 2 Calculated reaction free energy of hydrogen chemisorption as a function of hydrogen coverage: **a** differential free energy and **b** average free energy

to occur at certain H-coverage, where a-ΔG_H is close to zero (Fig. 2b). For example, if the VS_2 monolayer is fully covered by hydrogen atoms $\left(\frac{16}{16}\right)$ initially at $\varepsilon = 6$ %, the individual process starts first. When the H-coverage is reduced to $\frac{9}{16}$ (a-$\Delta G_H = 0.003$ eV), the collective process occurs because the total reaction energy in collective process (a-$\Delta G_H \times 9 = 0.027$ eV) is less than d-ΔG_H in individual process (0.07 eV). If the H-coverage on the VS_2 monolayer is less than $\left(\frac{8}{16}\right)$, initially, only individual process will happen. Similarly, the collective processes under $\varepsilon = 2$ and 10 % are more easier than individual processes at hydrogen coverages of $\frac{5}{16}$ and $\frac{14}{16}$, respectively. Generally, the strained VS_2 monolayer shows better catalytic performance than other TMDs monolayers and nanoribbons because of the near-zero Gibbs free energy in a wide range of hydrogen coverage.

To reveal the origin of H-coverage-dependent HER activity under tension, the density of state (DOS) is calculated. The carrier density can be estimated from the calculated DOSs. We see that the carrier density changes with the tension and hydrogen coverage (Fig. 3), which may indicate their effects on the HER activity in individual/collective process. At $\varepsilon = 2$ %, the VS_2 monolayer shows strong metallic characteristic with high free carrier density under the Fermi level at a hydrogen coverage of $\frac{3}{16}$, as indicated by the continuous DOS spectrum from −3 to 2.2 eV (Fig. 3a). With the increase of hydrogen coverage to $\frac{9}{16}$, the DOS spectrum separates into two regions with a small gap from −0.9 to −0.5 eV, and the free carrier density under the Fermi level is accordingly reduced (Fig. 3b). Further increasing hydrogen coverage to $\frac{16}{16}$, the DOS spectrum separates into three regions and the Fermi level is within the band gap, resulting in semiconducting characteristic and poor free carrier density. The reduction of carrier density with the increment of hydrogen coverage should be responsible for the reduction of HER performance (Fig. 2a). At the same time, we see that the DOS spectrum of VS_2 monolayer with a hydrogen coverage of $\frac{3}{16}$ under $\varepsilon = 6$ % is divided into two regions and the carrier density under the Fermi level is less than that under $\varepsilon =$

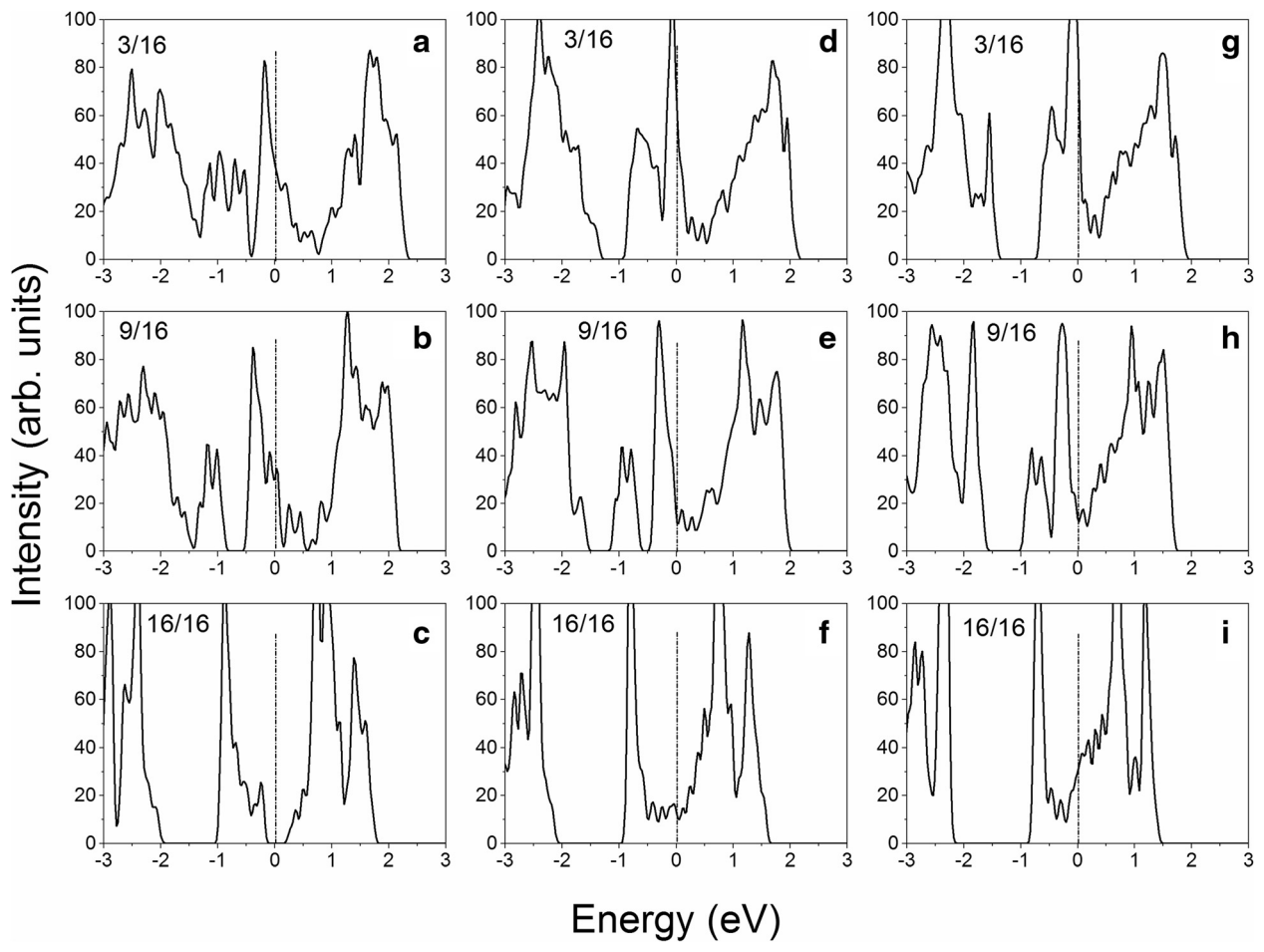

Fig. 3 Calculated total density of states of VS_2 monolayer under a tension of 2 % (**a**–**c**), 6 % (**d**–**f**), and 10 % (**g**–**i**) at a hydrogen coverage of 3/16, 9/16, and 16/16, respectively

2 % (Fig. 3d), leading to the reduction of HER activity. Further increasing the tension ($\varepsilon = 10$ %), the gap between two DOS regions is enlarged and the area under the Fermi level is reduced, indicating reduced carrier density and resulting in further reduction of HER activity, which is consistent with the calculated Gibbs free energies (Fig. 2a). Comparing the DOSs of VS_2 monolayers with a hydrogen coverage of 9/16 under $\varepsilon = 2$, 6, and 10 %, we see that the carrier density under the Fermi level increases as the tension increases (Figs. 3b, e, h), as indicated by the reduced/demolished gap around −0.5 eV, which is also consistent with the calculated Gibbs free energies (Fig. 2a). At full hydrogen coverage, we see that the HER activity of VS_2 monolayer is not significantly improved (Fig. 2a). The calculated DOSs show that the Fermi levels are within conduction bands (Fig. 3f, i). However, the strong sharp DOS peaks around −0.8 eV may indicate localized states, which may reduce the carrier density and increase charge recombination centers, leading to differentially removing hydrogen difficult (Fig. 2a).

Conclusions

We carry out first-principles to investigate the effects of tension on the hydrogen evolution reduction of VS_2 monolayer. We find that tension can tune the HER performance of VS_2 monolayer at different hydrogen coverage. The HER activity at high hydrogen coverage is greatly improved for both of individual and collective processes by increased tension. The hydrogen coverages for best HER performance in both individual and collective processes increase with the increment of tension. Generally, individual process is easier to occur in a wide range of hydrogen coverage, and collective process can happen at certain hydrogen coverage at the same tension. The optimal HER performance of VS_2 monolayer with near-zero Gibbs free energy, comparable to Pt, can be achieved by tuning tension. We further show that the change of HER performance at different hydrogen coverages and under various tensions is closely related to the carrier density. High free carrier density is responsible for the improved HER activity. During revision, we noticed that Li et al. recently reported that strain can enhance the catalytic activity of MoS_2 basal planes [51]. We see that the tension may provide an efficient way to modify the HER performance of VS_2 and other 2D monolayers and find applications to water electrolysis for hydrogen production.

Competing interests

The author declares that he has no competing interests.

Acknowledgements

Hui Pan thanks the support of the Science and Technology Development Fund from Macau SAR (FDCT-068/2014/A2, FDCT-132/2014/A3, and FDCT-110/2014/SB) and the Multi-Year Research Grant (MYRG2014-00159-FST and MYRG2015-00017-FST) from the Research and Development Office at the University of Macau. The DFT calculations were performed at the High Performance Computing Cluster (HPCC) of Information and Communication Technology Office (ICTO) at the University of Macau.

Received: 3 December 2015 Accepted: 9 February 2016
Published online: 29 February 2016

References

1. Cipriani G, Di Dio V, Genduso F, La Cascia D, Liga R, Miceli R, Galluzzo GR (2014) Perspective on hydrogen energy carrier and its automotive applications. Int J Hydrogen Energy 39:8482–8494
2. Andrews J, Shabani B (2014) The role of hydrogen in a global sustainable energy strategy. Willy Interdisciplinary Rev Energy Environ 3:474–489
3. Hisatomi T, Kubota J, Domen K (2014) Recent advances in semiconductors for photocatalytic and photoelectrochemical water splitting. Chem Soc Rev 43:7520–7535
4. Peng XN, He C, Fan X, Liu QY, Zhang J, Wang H (2014) Photovoltaic devices in hydrogen production. Int J Hydrogen Energy 39:14166–14171
5. Christopher K, Dimitrios R (2012) A review on energy comparison of hydrogen production methods from renewable energy sources. Energy Environ Sci 5:6640–6651
6. Vedarajan R, Ikeda S, Matsumi N (2014) Electrochemical characterization of TiO2/WOx nanotubes for photocatalytic application. Nanoscale Res Lett 9:573
7. Chen WF, Muckerman JT, Fujita E (2013) Recent developments in transition metal carbides and nitrides as hydrogen evolution electrocatalysts. Chem Commun 49:8896–8909
8. Contreras JL, Salmones J, Colin-Luna JA, Nuno L, Quintana B, Cordova I, Zeifert B, Tapia C, Fuentes GA (2014) Catalysts for H_2 production using the ethanol steam reforming: a review. Int J Hydrogen Energy 39:18835–18853
9. Dou BL, Song YC, Wang C, Chen HS, Yang MJ, Xu YJ (2013) Hydrogen production by enhanced-sorption chemical looping steam reforming of glycerol in moving-bed reactors. Appl Energy 130:342–349
10. Sun RY, Li YJ, Zhao JL, Liu CT, Lu CM (2013) CO_2 capture using carbide slag modified by propionic acid in calcium looping process for hydrogen production. Int J Hydrogen Energy 38:13655–13663
11. Tavangar A, Tan B, Venkatakrishnan K (2013) Sustainable approach toward synthesis of green functional carbonaceous 3-D micro/nanostructures from biomass. Nanoscale Res Lett 8:348
12. Lu XH, Xie SL, Yang H, Tong YX, Ji HB (2014) Photoelectrochemical hydrogen production from biomass derivatives and water. Chem Rev Soc 43:7581–7593
13. Carmo M, Fritz DL, Merge J, Stolten D (2013) A comprehensive review on PEM water electrolysis. Int J Hydrogen Energy 38:4901–4934
14. Yuan XX, Hu XX, Ding XL, Kong HC, Sha HD, Lin H, Wen W, Shen GX, Guo Z, Ma ZF, Yang Y (2013) Effects of cobalt precursor on pyrolyzed carbon-supported cobalt-polypyrrole as electrocatalyst toward oxygen reduction reaction. Nanoscale Res Lett 8:478
15. Morales-Guio CG, Stern LA, Hu XL (2014) Nanostructured hydrotreating catalysts for electrochemical hydrogen evolution. Chem Soc Rev 43:6555–6569
16. Fang YH, Liu ZP (2009) Surface phase diagram and oxygen coupling kinetics on flat and stepped Pt surfaces under electrochemical potentials. J Phys Chem C 113:9765–9772
17. Lu YZ, Jiang YY, Chen W (2013) PtPd porous nanorods with enhanced electrocatalytic activity and durability for oxygen reduction reaction. Nano Energy 2:836–844
18. Gressley J, Jarmaillo TF, Bonde J, Chorkendorff I, Nørskov JK (2006) Computational high-throughput screening of electrocatalytic materials for hydrogen evolution. Nat Mater 5:909–913
19. Pan H, Feng YP, Lin JY (2010) Enhancement of hydrogen evolution on tungsten doped platinum. J Comput Theor Nanosci 7:547–551
20. Fang YH, Wei GF, Liu ZP (2013) Catalytic role of minority species and minority sites for electrochemical hydrogen evolution on metals: surface charging, coverage, and Tafel kinetics. J Phys Chem C 117:7669–7680
21. Yung TY, Liu TY, Huang LY, Wang KS, Tzou HM, Chen PT, Chao CY, Liu LK (2015) Characterization of Au and bimetallic PtAu nanoparticles on PDDA-graphene sheets as electrocatalysts for formic acid oxidation. Nanoscale Res Lett 10:365
22. Xia BY, Wu HB, Li N, Yan Y, Lou XW, Wang X (2015) One-pot synthesis of Pt-Co alloy nanowire assemblies with tunable composition and enhanced electrocatalytic properties. Angew Chem Int Ed 54:3797–3801

23. Kibsgaard J, Chen Z, Reinecke BN, Jaramillo TF (2012) Engineering the surface structure of MoS2 to preferentially expose active edge sites for electrocatalysis. Nat Mater 11:963–969
24. Qu Y, Pan H, Kwok CT, Wang ZS (2015) A first-principles study on hydrogen evolution reaction of VS_2 nanoribbons. Phys Chem Chem Phys 17:24820–24825
25. Yang J, Shin HS (2014) Recent advances in layered transition metal dichalcogenides for hydrogen evolution reaction. J Mater Chem A 2:5979–5985
26. Qu Y, Pan H, Kwok CT, Wang ZS (2015) Effect of doping on hydrogen evolution reaction of vanadium disulfide monolayer. Nanoscale Res Lett 10:480
27. Saadi FH, Carim AI, Velazquez JM, Baricuatro JH, McCrory CCL, Soriaga MP, Lewis NS (2014) Operando synthesis of macroporous molybdenum diselenide films for electrocatalysis of the hydrogen-evolution reaction. ACS Catal 4:2866–2873
28. Xu K, Wang FM, Wang ZX, Zhan XY, Wang QS, Cheng ZZ, Safdar M, He J (2014) Component-controllable $WS_{2(1-x)}Se_{2x}$ nanotubes for efficient hydrogen evolution reaction. ACS Nano 8:8468–8476
29. Chen TY, Chang YH, Hsu CL, Wei KH, Chiang CY, Li LJ (2013) Comparative study on MoS_2 and WS_2 for electrocatalytic water splitting. Int J Hydro Energy 38:12302–12309
30. Lukowski MA, Daniel AS, English CR, Meng F, Forticaux A, Hamers RJ, Jin S (2014) Highly active hydrogen evolution catalysis from metallic WS_2 nanosheets. Energy Environ Sci 7:2608–2613
31. Lin J, Peng ZW, Wang G, Zakhidov D, Larios E, Yacaman MJ, Tour JM (2014) Enhanced electrocatalysis for hydrogen evolution reactions from WS_2 nanoribbons. Adv Fun Mater 4:1301875
32. Pan H (2014) Metal dichalcogenides monolayers: novel catalysts for electrochemical hydrogen production. Sci Rep 4:5348
33. Voiry D, Salehi M, Silva R, Fujita T, Chen MW, Asefa T, Shenoy VB, Eda G, Chhowalla M (2014) Conducting MoS_2 nanosheets as catalysts for hydrogen evolution reaction. Nano Lett 13:6222–6227
34. Lukowski MA, Daniel AS, Meng F, Forticaux A, Li LS, Jin S (2013) Enhanced hydrogen evolution catalysis from chemically exfoliated metallic MoS_2 nanosheets. J Am Chem Soc 135:10274–10277
35. Shi JP, Ma DL, Han GF, Zhang Y, Ji QQ, Gao T, Sun JY, Song XJ, Li C, Zhang YS, Lang XY, Zhang YF, Liu ZF (2014) Controllable growth and transfer of monolayer MoS_2 on Au foils and its potential application in hydrogen evolution reaction. ACS Nano 8:10196–10204
36. Geng XM, Wu W, Li N, Sun WW, Armstrong J, Al-hilo A, Brozak M, Cui JB, Chen TP (2014) Three-dimensional structures of MoS_2 nanosheets with ultrahigh hydrogen evolution reaction in water reduction. Adv Fun Mater 24:6123–6129
37. Zhang XW, Meng F, Christianson JR, Arroyo-Torres C, Lukowski MA, Liang D, Schmidt JR, Jin S (2014) Vertical heterostructures of layered metal chalcogenides by van der Waals epitaxy. Nano Lett 14:3047–3052
38. Voiry D, Yamaguchi H, Li JW, Silva R, Alves DCB, Fujita T, Chen MW, Asefa T, Shenoy VB, Eda G, Chhowalla M (2013) Enhanced catalytic activity in strained chemically exfoliated WS_2 nanosheets for hydrogen evolution. Nat Mater 13:850–855
39. Yu YF, Huang SY, Li YP, Steinmann SN, Yang WT, Cao LY (2014) Layer-dependent electrocatalysis of MoS_2 for hydrogen evolution. Nano Lett 14:553–558
40. Yan Y, Xia BY, Xu ZC, Wang X (2014) Recent development of molybdenum sulfides as advanced electrocatalysts for hydrogen evolution reaction. ACS Catal 4:1693–1705
41. Tsai C, Chan K, Nørskov JK, Abild-Pedersen F (2015) Rational design of MoS2 catalysts: tuning the structure and activity via transition metal doping. Catal Sci Technol 5:246–253
42. Tsai C, Abild-Pedersen F, Nørskov JK (2014) Tuning the MoS_2 edge-site activity for hydrogen evolution via support interactions. Nano Lett 14:1381–1387
43. Lee JH, Jang WS, Han SW, Baik HK (2014) Efficient hydrogen evolution by mechanically strained MoS2 nanosheets. Langmuir 30:9866–9873
44. Hohenberg P, Kohn W (1964) Inhomogeneous electron gas. Phys Rev 136: B864–B871
45. Blöchl PE (1994) Projector augmented-wave method. Phys Rev B 50:17953–17979
46. Kresse G, Furthmuller J (1996) Efficient iterative schemes for ab initio total-energy calculations using a plane-wave basis set. Phys Rev B 54:11169–11186
47. Perdew JP, Burke K, Ernzerhof M (1996) Generalized gradient approximation made simple. Phys Rev Lett 77:3865–3868
48. Kresse G, Joubert D (1999) From ultrasoft pseudopotentials to the projector augmented-wave method. Phys Rev B 59:1758–1775
49. Monkhorst HJ, Pack J (1976) Special points for brillouin-zone integrations. Phys Rev B 13:5188–5192
50. Pan H (2014) Electronic and magnetic properties of vanadium dichalcogenides monolayers tuned by hydrogenation. J Phys Chem C 118: 13248–13253
51. Li H, Tsai C, Koh AL, Cai L, Contryman AW, Fragapane AH, Zhao JH, Han HS, Manoharan HC, Abild-Pedersen F, Nørskov JK, Zheng XL (2016) Activating and optimizing MoS_2 basal planes for hydrogen evolution through the formation of strained sulphur vacancies. Nat Mater 15:48–53